ACS APPLIED MATERIALS & INTERFACES

Research Article

www.acsami.org

Electrocatalytic Hydrogen Evolution from Molybdenum Sulfide–Polymer Composite Films on Carbon Electrodes

Youssef Lattach, Alain Deronzier, and Jean-Claude Moutet*

Université Joseph Fourier Grenoble 1, Département de Chimie Moléculaire, UMR CNRS-5250, Institut de Chimie Moléculaire de Grenoble, FR CNRS-2607, BP 53, 38041 Cedex 9, Grenoble, France

Supporting Information

ABSTRACT: The design of more efficient catalytic electrodes remains an important objective for the development of water splitting electrolyzers. In this context a structured composite cathode material has been synthesized by electrodeposition of molybdenum sulfide (MoS_x) into a poly(pyrrole-alkylammonium) matrix, previously coated onto carbon electrodes by oxidative electropolymerization of a pyrrole-alkylammonium monomer. The composite material showed an efficient electrocatalytic activity toward proton reduction and the hydrogen evolution reaction (HER). Data from Tafel plots have demonstrated that the electron transfer rate in the composite films is fast, in agreement with the high catalytic activity of this cathode material. Bulk electrolysis of acidic water at carbon foam electrodes modified with the composite have shown that the cathodes display a high catalytic activity and a reasonable operational stability, largely exceeding that of regular amorphous MoS_x electrodeposited on naked carbon foam. The enhanced catalytic performances of the composite electrode material were attributed to the structuration of the composite, which led to a homogeneous distribution of the catalyst on the carbon foam network, as shown by SEM characterizations.

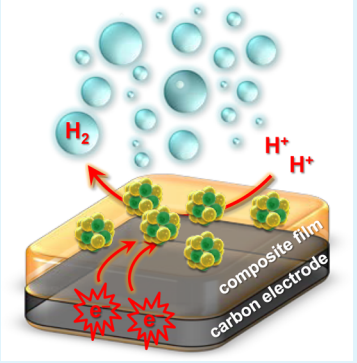

KEYWORDS: *electrocatalysis, catalytic cathode, hydrogen evolution reaction, molybdenum sulfide, functionalized polypyrrole, nanocomposites*

INTRODUCTION

Conversion of clean and renewable energy sources to hydrogen via splitting of water offers an appealing solution toward energy and environmental issues.[1] One of the critical steps in the water splitting process is the hydrogen evolution reaction (HER), which requires the employment of catalysts. So far, platinum group metals are considered as the most effective electrocatalysts for HER,[2] but severely suffer from their rarity and high cost. Thus, the need for efficient non-noble, earth abundant catalysts is critical. Among them, molybdenum-based materials, especially molybdenum sulfides, appear as promising HER catalysts and represent a very promising alternative to noble metals.[3−6] Molybdenum sulfide (named MoS_x herein), in the form of electrodeposited,[7,8] drop-casted,[9] or spin-coated[10] amorphous films, nanoparticles assembled on gold,[11,12] carbon paper,[13] glassy carbon,[14] and FTO[14] surfaces, have been reported for their high electrocatalytic activity toward hydrogen evolution in acidic electrolytes. Increased electrocatalytic activity and stability has been obtained by incorporating MoS_x into various templates or supports, including reduced graphene oxide,[15] mesoporous graphene foam[16] and carbon nanospheres,[17] carbon black particles,[18] carbon fibers,[19] or MoO_3 nanowires[20] networks. The enhanced activity of these MoS_x-based hybrid and composite materials is believed to be due to the increase of the active surface area. Moreover, aggregation of catalyst particles, which results in a decrease of activity, can be in principle prevented by using a matrice or a support.

Surprisingly, so far the synthesis of MoS_x-polymer composites remains limited to a very few examples,[21−25] despite this approach providing an attractive versatility in the controlled synthesis of structured assemblies of catalysts particles with functionalized polymers.[26] Bélanger and coworkers have described the preparation of polypyrrole-molybdenum sulfide composite thin films, electrodeposited on electrodes from aqueous solutions containing pyrrole and ammonium tetrathiomolybdate.[21−23] Characterization by elemental analysis and X-ray absorption spectroscopy of the materials synthesized in this way has demonstrated that the composite films contained both MoS_3 and MoS_4^{2-} species.[22] They have recently been found very active for HER in acidic electrolyte, but have shown a poor stability.[25]

We reported earlier that the use of polypyrrole films functionalized by cationic moieties provides a straightforward and efficient route for the electrosynthesis of nanostructured composite electrode materials containing a dispersion of various metal and metal oxide catalysts,[27−34] which exhibit high activity for numerous electrocatalytic applications. Very recently we have described the synthesis of a photocathode, by

Received: April 13, 2015
Accepted: July 6, 2015
Published: July 6, 2015

DOI: 10.1021/acsami.5b03188
ACS Appl. Mater. Interfaces 2015, 7, 15866−15875

electrodeposition of MoS_x as HER catalyst into a photosensitive poly[pyrrole-Ru(2,2′-bipyridine)$_3^{2+}$)] film. This composite electrode material exhibited a stable photocatalytic activity for hydrogen evolution under visible light in acidic aqueous electrolytes.[35] Following a similar synthetic strategy, here we report the fabrication of a simpler structured molybdenum sulfide-based cathode material for HER. The composite was synthesized by incorporation of tetrathiomolybdate anions by ion-exchange into a poly(pyrrole-alkylammonium) thin film, followed by electroreduction of trapped MoS_4^{2-} species to precipitate molybdenum sulfide in the polymer matrix. The electrocatalytic activity of this electrode material has been evaluated toward water reduction and the hydrogen evolution reaction. Furthermore, bulk electrocatalytic reduction of water at large surface carbon foam modified electrodes has demonstrated that the composite films display a higher catalytic activity and a good operational stability, largely exceeding that of regular electrodeposited amorphous molybdenum sulfide.

2. EXPERIMENTAL SECTION

2.1. Chemicals and Reagents. Ammonium tetrathiomolybdate ($(NH_4)_2MoS_4$, 99.95%, Aldrich), tetraethylammonium chloride (Et_4NCl, Fluka), dichloromethane (CH_2Cl_2), acetonitrile (CH_3CN, ACROS, HPLC grade), sodium perchlorate ($NaClO_4$), and tetra-*n*-butylammonium perchlorate (TBAP, Fluka puriss) were used as received. Purification of water (15.0 MΩ cm, 24 °C) was performed using a milli-Q system (Purelab option, Elga). Reference gas (1% and 5% H_2 in N_2, Air Liquide) were purchased from commercial suppliers. (3-Pyrrol-1-ylpropyl)triethylammonium tetrafluoroborate, denoted monomer **1** (Scheme 1), was prepared according to a previously reported procedure.[30]

Scheme 1. Pyrrole-Containing Monomer (1) Used in This Work

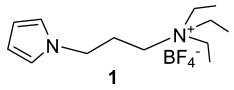

1

Tetraethylammonium tetrathiomolybdate ($(Et_4N)_2MoS_4$) was prepared according to a literature procedure.[36] The reaction was performed under argon. To a suspension of $(NH_4)_2MoS_4$ (200 mg, 0.77 mmol) in CH_3CN (11 mL) was added Et_4NCl (267 mg, 1.61 mmol). The red mixture was stirred at room temperature for 2.5 h. The volume of solution was then reduced to 1 mL under vacuum, and the resulting red precipitate was filtered off, washed with CH_2Cl_2 (3 × 10 mL), and dried under vacuum. $(Et_4N)_2MoS_4$ was isolated as a bright red solid (236 mg, 63%).

2.2. Electrodes, Electrochemical Cells, and Instrumentation. All electrochemical experiments were performed using a conventional three-electrode system. Electroanalytical experiments were performed using a CHI 660B electrochemical analyzer (CH Instruments). Electrosynthesis of carbon foam modified electrodes and bulk electrolysis were carried out using an EGG PAR model 273 potentiostat. Potentials were referred to the Ag|AgCl (3 M KCl) or to the Ag|Ag$^+$ (10 mM in CH_3CN + 0.1 M TBAP) reference electrodes in aqueous and non aqueous electrolytes, respectively. In some cases potentials were referred to the reversible hydrogen electrode (RHE) by adding a value of (0.205 + 0.059 × pH) V. For analytical experiments, glassy carbon working microelectrodes (3 mm diameter) were polished with 1-μm diamond paste. Large scale electrolysis was conducted on modified carbon foam electrodes (0.8 cm^3, porosity 100 ppi, from Electrosynthesis). Samples for atomic force microscopy studies were deposited onto indium tin oxide (ITO) electrodes. All experiments were conducted at room temperature under an argon atmosphere.

2.3. Preparation of the Nanocomposite Film Modified Electrodes. *Electrosynthesis of Poly(Pyrrole-alkylammonium) Film Modified Electrodes.* Polymer films (denoted poly**1**) were grown by potentiostatic oxidative electropolymerization in unstirred solutions of monomer **1** (4 mM) in CH_3CN containing TBAP (0.1 M) as supporting electrolyte.[28,30] The extent of the polymerization was controlled through the anodic charge recorded during electrolysis. The amount of pyrrole units in the films, and thus the apparent surface coverage in ammonium units Γ_{N+} (mol cm^{-2}) were determined, after transfer of the modified electrodes into monomer-free CH_3CN electrolyte, from the integration of the polypyrrole oxidation wave recorded at low scan rate (10 mV s^{-1}), assuming that one in three pyrrole units is oxidized.[37] Thin films with Γ_{N+} ranging from 2.0 × 10^{-8} mol cm^{-2} to 6.0 × 10^{-8} mol cm^{-2} were grown onto glassy carbon disc (3 mm diameter) electrodes by controlled potential oxidation carried out at E_{app} = 0.85 V vs Ag|Ag$^+$ 10^{-2} M, using polymerization charges from 0.5 to 2 mC. Modification of carbon foam electrodes was achieved by potentiostatic oxidative electropolymerization of monomer **1** in acetonitrile in the same experimental conditions as described above, using polymerization charges of 0.5 to 1.5 C. This process led to the deposition of a polymeric material onto the carbon foam containing about 1 to 3 μmol of ammonium groups (electrodeposition yield around 45%).

*Electrodeposition of MoS_x in Poly-**1** Films.* The electrodeposition of molybdenum sulfide onto poly-**1** films was performed following three different processes: (i) repeated cyclic voltammetry scans of the poly**1** film modified electrodes over the 0.1 to −1.0 V potential range in a 10 mM aqueous solution of $(NH_4)_2MoS_4$ containing 0.1 M $NaClO_4$ (pH 6.6); (ii) incorporation of MoS_4^{2-} anions by ion-exchange into poly**1** films upon soaking for 10 min in a 2 mM solution of $(Et_4N)_2MoS_4$ in CH_3CN, followed by repeated CV scans over the 0.1 to −1.2 V potential range in clean 0.1 M aqueous $NaClO_4$ electrolyte (pH 6); (iii) same procedure as above, but the incorporation by anion-exchange of MoS_4^{2-} into poly**1** films was preformed by soaking the poly**1** film modified electrodes into a 10 mM aqueous solution of $(NH_4)_2MoS_4$.

For comparative studies, MoS_x films were coated onto naked carbon and ITO electrodes by repeated CV scans (typically 25 cycles) over the 0.1 to −1.0 V potential range in a 10 mM aqueous solution of $(NH_4)_2MoS_4$ containing 0.1 M $NaClO_4$ (pH 6.6).

2.4. Atomic Force Microscopy Experiments. Samples for atomic force microscopy (AFM) measurements were prepared by electrodeposition of MoS_x on poly**1** films-coated ITO-coated glass electrodes (1 cm^2). Electropolymerization of monomer **1** in acetonitrile electrolyte was performed at a controlled oxidation potential of 1.1 V vs Ag|Ag$^+$ 10^{-2} M, (Γ_{N+} = 2.17 × 10^{-8} mol cm^{-2}). MoS_x was then electrodeposited onto poly**1** films, by incorporation of MoS_4^{2-} 10 mM in CH_3CN, followed by repeated cyclic voltammetry scans in clean 0.1 M $NaClO_4$ (pH 6). For comparative studies MoS_x was deposited onto a naked ITO electrode by cycling in 10 mM aqueous

DOI: 10.1021/acsami.5b03188
ACS Appl. Mater. Interfaces 2015, 7, 15866−15875

solution of $(NH_4)_2MoS_4$ containing 0.1 M $NaClO_4$ (pH 6.6). AFM measurements were performed with a PicoPlus instrument (Molecular Imaging) equipped with a PicoScan controller and an AC-mode control box. The topography images were recorded with different scanning ranges and a tapping mode probe was used for imaging. AFM cantilevers with an aluminum coating (BudgetSensors Tap150Al-G) with a nominal spring constant of 5 N m^{-1} were used. The measurement frequency was set to 15% below the resonance frequency (about 150 kHz). Images were treated using Gwyddion program.

2.5. Scanning Electron Microscopy. Scanning electron microscopy (SEM) images of modified carbon foam electrodes were obtained using a Zeiss FEG-SEM microscope equipped with a Bruker AXS X-ray analyzer (EDX) and a silicon drift detector (SDD; 30 mm^2 of active surface); data were treated with the QUANTA software.

2.6. Analysis of Hydrogen Production. The amount of hydrogen evolved was quantified from an analysis of the gas mixture in the headspace of the electrochemical cell (sampling of 100 μL of gas) by gas chromatography (PerkinElmer Autosystem XL Gas Chromatograph equipped with a 5 Å molecular sieve column (oven temperature = 303 K) and a thermal conductivity detector (TCD), using argon as carrier gas. Prior to each experiment, GC/TCD calibration was carried out with two samples of the reference gas (1% and 5% H_2 in N_2).

The number of moles (n_{H_2}) and the volume (V_{H_2}) of hydrogen produced was calculated according to eqs 1 and 2, respectively.

$$n_{H_2}\,(\text{mol}) = \frac{\text{detected peak area}}{\text{calibration peak area}} \times 0.01 \times \frac{\text{headspace volume [L]}}{24.5\ [\text{L mol}^{-1}]} \quad (1)$$

$$V_{H_2}\,(\text{L}) = \frac{\text{detected peak area}}{\text{calibration peak area}} \times 0.01 \times \text{headspace volume [L]} \quad (2)$$

where 0.01 is the reference percentage of H_2 in N_2 (corresponding to 1% of H_2 in N_2) which is linked to the calibration peak area, 24.5 L mol^{-1} is the molar volume of an ideal gas at a temperature of 298.15 K and pressure of 101325 Pa. For all experiments, the overpressure in the cell (headspace volume 175 mL) due to the hydrogen produced was regarded as negligible, since the total amount of hydrogen produced did not exceed 15 mL. The turnover number related to the catalyst (TON) was calculated according to eq 3

$$\text{TON} = \frac{n_{H_2}}{n_{Cat}} \quad (3)$$

where n_{H_2} is the number of moles of hydrogen produced and n_{Cat} is the number of moles of catalyst in the composite film. We consider that one mole of catalyst gives 1 mol of H_2.

RESULTS AND DISCUSSION

3.1. Electrosynthesis of Poly(Pyrrole-alkylammonium)-molybdenum Sulfide Nanocomposite Electrode Materials. It is now well-established that amorphous molybdenum sulfide films can be deposited under various electrochemical conditions[7] from aqueous solution of ammonium tetrathiomolybdate, onto carbon, platinum, or conducting oxide-coated glass electrodes.[7,8,22,38,39] In particular, thin films of MoS_x are readily cathodically electrodeposited from MoS_4^{2-} aqueous solutions[7,22,39] (see for example Figure S1A in Supporting Information). These amorphous materials have been shown to be efficient hydrogen evolution electrocatalysts in acidic aqueous electrolytes[5,7,8] (see Figure S1B in Supporting Information). With a view to developing structured, active and stable catalytic cathodes for HER, we have studied the synthesis of MoS_x-polymer composite electrode materials. As pointed out in the introduction, we used the general strategy already described by our group for the preparation of composite electrode materials, based on the electroprecipitation of catalyst particles into functionalized polypyrrole thin films coated onto carbon electrodes.[27−35]

First, we have studied the electroprecipitation of MoS_x into poly(pyrrole-alkylammonium) thin films, simply by scanning C|poly**1** film modified electrodes over the 0.1 to −1.0 V potential range in a $(NH_4)_2MoS_4$ aqueous solution. The CV features (Figure 1A) are similar to those observed in the same experimental conditions at a naked carbon electrode (see Figure S1A in Supporting Information). This is consistent with the electroprecipitation of molybdenum sulfide into the polyammonium film, although the amount of deposited MoS_x is obviously lower than that deposited on a naked carbon in the same experimental conditions, as evidenced from the significantly smaller redox wave observed for the composite film modified electrode. However, the polarization curve recorded in an acidic aqueous electrolyte (Figure 1C, curve a) shows that the modified electrode synthesized in this way displays a high catalytic activity for hydrogen evolution, similar to that obtained with a C|MoS_x modified electrode (Supporting Information Figure S1B, curve a), thereby confirming the effective synthesis of a poly**1**-MoS_x catalytic electrode material.

Nevertheless, we found this strategy to synthesize polymer-MoS_x composite films poorly reproducible, because of the fast degradation of the deposition bath during the electrodeposition of molybdenum sulfide due to a strong precipitation in the electrolyte of sulfur and sulfide species.[7,37]

Thus, we designed a clean, reproducible and less material-consuming strategy for the electrosynthesis of molybdenum sulfide-based composite materials, taking advantage of the excellent ion-exchange properties of the cationic poly**1** films, and of the well-behaved redox activity of MoS_4^{2-} in organic electrolytes. This strategy is summarized in Scheme 2.

The tetrathiomolybdate anion is characterized by a reversible, one-electron reduction wave in organic electrolytes[40,41] ($E_{1/2}$ = −2.69 V vs Ag|Ag^+ 10^{-2} M for the $Mo^{VI}S_4^{2-}/Mo^{V}S_4^{3-}$ redox couple in acetonitrile +0.1 M TBAP; Figure 2A, curve a; see also Figure S2 in Supporting Information). Immersion of C|poly-**1** modified electrodes in the solution of $(Et_4N)_2MoS_4$ in acetonitrile leads to the binding of the tetrathiomoybdate dianion in the polymer matrix by anion exchange with ClO_4^-. The incorporation of intact MoS_4^{2-} in the poly(pyrrole-alkylammonium) film was established by cyclic voltammetry. Cyclic voltammograms recorded on C|poly-**1** electrodes in 2 mM $(Et_4N)_2MoS_4$ in CH_3CN show two reversible redox peak systems at about −2.5 and −2.7 V (Figure 2A, curve b). The redox potential for the last wave lies not far away from that observed for MoS_4^{2-} in homogeneous solution at a bare carbon electrode. This wave disappears if the modified electrode is thoroughly rinsed and transferred to clean acetonitrile +0.1 M TBAP electrolyte (Figure 2B). The voltammogram then shows

DOI: 10.1021/acsami.5b03188
ACS Appl. Mater. Interfaces 2015, 7, 15866−15875

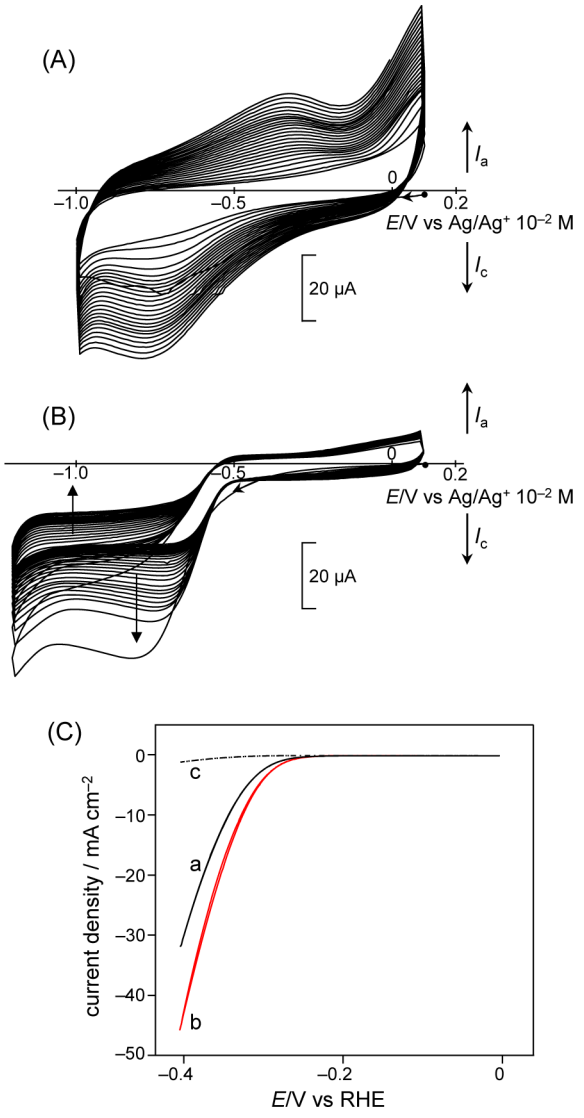

Figure 1. (A) Electroreductive precipitation of MoS_x into a poly(pyrrole-alkylammonium) film by repeated cyclic voltammetry (CV) scans (25 cycles; scan rate 50 mV s^{-1}) at a C|poly**1** modified electrode (3 mm diameter; $\Gamma_{N+} = 8 \times 10^{-8}$ mol cm^{-2}) in a 10 mM aqueous solution of $(NH_4)_2MoS_4$ containing 0.1 M $NaClO_4$, pH 6.6. (B) Repeated CV scans (25 cycles; scan rate 50 mV s^{-1}) in 0.1 M aqueous $NaClO_4$ (pH 6), recorded at a C|poly**1** modified electrode (3 mm diameter; $\Gamma_{N+} = 8 \times 10^{-8}$ mol cm^{-2}) previously soaked for 10 min in a 2 mM solution of $(Et_4N)_2MoS_4$ in CH_3CN. (C) Polarization curves recorded in aqueous H_2SO_4 (pH 0.3) with the C|poly**1**-MoS_x modified electrodes prepared in A (curve a) and B (curve b); curve c is recorded at a C|poly**1** modified electrode without incorporation of MoS_x; scan rate 20 mV s^{-1}.

a single wave ($E_{1/2}$ = −2.50 V vs. Ag|Ag^+ 10^{-2} M) characteristic of the tetrathiomolybdate anion entrapped in the polymer film. The peaks currents are significantly higher than those recorded at a bare carbon electrode (Figure 2A, curve a), which demonstrates that MoS_4^{2-} species are concentrated and retained by poly-**1**, presumably by electrostatic binding.

The anion-exchange and binding properties of poly-**1** films have already been largely evidenced using various anionic redox probes, such as ferrocyanide[30] or iron−sulfur clusters.[42] The binding of the tetrathiomolybdate in the polyammonium matrix considerably perturbs its reduction potential. The half-wave potential for the electrostatically bound $Mo^{VI}S_4^{2-}/Mo^{V}S_4^{3-}$ redox couple (−2.50 V) is about 190 mV less negative than that measured for the free anion. The perturbation of the redox potential probably owes its origin to the electrostatic interaction of the tetrathiomolybdate anions with the cationic alkylammonium groups of the polymer film. Such behavior has already been observed for other redox anions bound to poly-**1** film modified electrodes.[30,42]

The incorporation ratio of MoS_4^{2-} in poly-**1** films has been defined as twice the ratio Γ_{Mo}/Γ_{N+}, where Γ_{Mo} and Γ_{N+} are the apparent surface coverages (mol cm^{-2}) in molybdate species and ammonium units, respectively, and taking into account that the dianionic tetrathiomolybdate must be bound to two monocationic alkylammonium groups of the film. Γ_{N+} was determined from the charge recorded under the polypyrrole oxidation wave (Figure 2A, curve c), and Γ_{Mo} was measured from the charge under the MoS_4^{2-}/MoS_4^{3-} reduction wave after transfer of the modified electrode into a clean electrolyte (Figure 2B). In our experimental conditions, the incorporation ratio was in the 66% to 50% range in poly-**1** films with Γ_{N+} ranging from 5×10^{-8} to 3×10^{-7} mol cm^{-2}.

The modified electrodes were then subjected to repeated CV scans (25 cycles; scan rate 50 mV s^{-1}) over the 0.1 to −1.2 V potential range in 0.1 M aqueous $NaClO_4$ electrolyte (pH 6), to precipitate MoS_x into the polymer matrix (see Figure 1B) by reduction of the tetrathiomolybdate anions trapped in the poly(pyrrole-alkylammonium) matrix. Polarization curves recorded in an acidic aqueous electrolyte have demonstrated the high catalytic activity toward proton reduction of the modified electrodes synthesized in this way (see for example Figure 1C, curve b), even higher than that obtained with the cathodes prepared by scanning C|poly-**1** film modified electrodes in an aqueous $(NH_4)_2MoS_4$ solution (Figure 1C, curve a). This observation confirms the efficient synthesis of C|poly-**1**-MoS_x modified electrodes using the anion exchange-electroprecipitation technique. It should also be emphasized that the amount of MoS_x precipitated into the polymer films can be easily estimated from the amount of MoS_4^{2-} incorporated by ion-exchange in poly-**1** films, previously determined from cyclic voltammetry experiments performed in acetonitrile (see above).

The incorporation of MoS_4^{2-} by anion exchange in poly-**1** films was also performed using a 10 mM $(NH_4)_2MoS_4$ aqueous solution. In this case the amount of tetrathiomolybdate anions effectively bound to the polyammonium matrix could also be determined from CV experiments, after thorough rinsing and transfer of the modified electrodes to clean acetonitrile +0.1 M TBAP electrolyte. The incorporation from aqueous solution of 10 mM $(NH_4)_2MoS_4$ in thin poly-**1** films is very similar (around 60%) to that obtained by using a solution of 2 mM $(NEt_4)_2MoS_4$ in acetonitrile. The precipitation of MoS_x into the polymer matrix by reduction of the tetrathiomolybdate anions incorporated from aqueous solution, upon repeated CV scans (see Figure S3A in Supporting Information) in acidic aqueous electrolyte, led to the formation of cathodes that displayed a catalytic activity for hydrogen evolution similar to that obtained by perfoming the anion exchange in an organic solution of tetrathiomolybdate (Figure S3B in Supporting Information).

As for the electrosynthesis of pure amorphous molybdenum sulfide films from aqueous solutions of ammonium tetrathiomolybdate,[7,38,39] we have considered various electrochemical conditions for the precipitation of MoS_x from entrapped MoS_4^{2-} in poly-**1** films, including potential cycling in the

DOI: 10.1021/acsami.5b03188
ACS Appl. Mater. Interfaces 2015, 7, 15866−15875

Scheme 2. General Strategy for the Electrosynthesis of Poly(Pyrrole-alkylammonium)-MoS_x Composite Film Modified Electrodes[a]

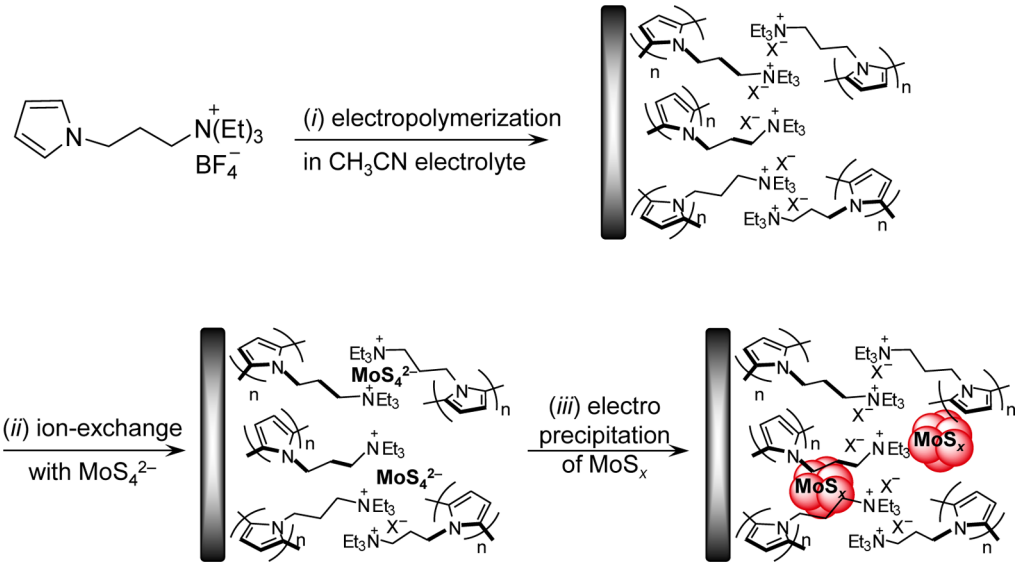

[a](i) Oxidative electropolymerization of monomer **1** (4 mM) in CH_3CN containing 0.1 M TBAP; (ii) incorporation of MoS_4^{2-} by ion-exchange into poly**1** upon soaking in a 2 mM CH_3CN solution of $(Et_4N)_2MoS_4$, or a 10 mM aqueous solution of $(NH_4)_2MoS_4$; (iii) electroprecipitation of MoS_x into poly-**1** by repeated CV scans over the 0.1 to −1.2 V potential range in 0.1 M aqueous $NaClO_4$ electrolyte (pH 6).

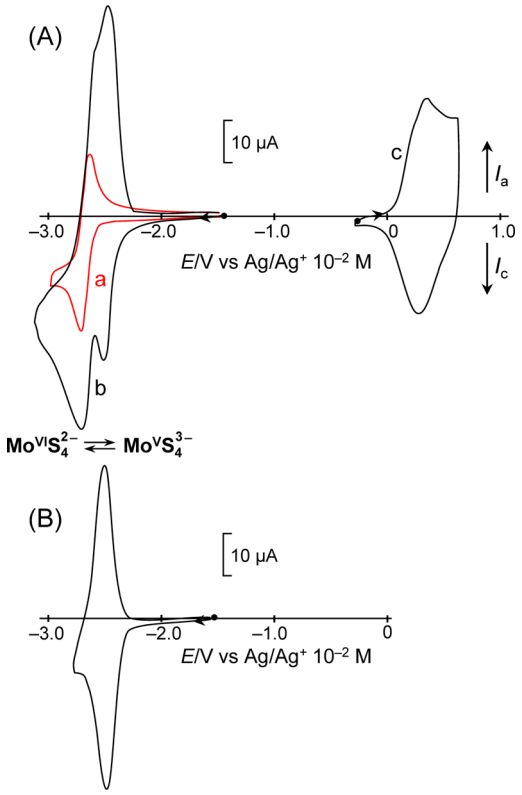

Figure 2. (A) CV curves recorded in CH_3CN containing 2 mM $(Et_4N)_2MoS_4$ and 0.1 M TBAP at a naked carbon disc (3 mm diameter) electrode (curve a), and at a C|poly-**1** electrode (curve b) (3 mm diameter; $\Gamma_{N+} = 9.5 \times 10^{-8}$ mol cm^{-2}); (curve c) CV curve for C|poly-**1** electrode recorded in clean CH_3CN + 0.1 M TBAP. (B) CV curve for the same C|poly-**1** modified electrode soaked for 10 min in the $(Et_4N)_2MoS_4$ solution and transferred to clean CH_3CN + 0.1 M TBAP electrolyte ($\Gamma_{N+} = 9.5 \times 10^{-8}$ mol cm^{-2}, $\Gamma_{Mo} = 3.2 \times 10^{-8}$ mol cm^{-2}). Scan rate = 50 mV s^{-1}.

negative potential region, anodic electrolysis at 0.1 V, and cathodic electrolysis at −1.0 V. It appeared that the composite film prepared by potential cycling were the more active, as evidenced from the polarization curves recorded in acidic electrolyte (see Figure S4 in Supporting Information). This method was thus chosen for the synthesis of catalytic cathodes used for further study of HER at the analytical and preparative scales.

3.2. Characterization of Poly(Pyrrole-alkylammonium)-MoS_x Composite Films. The effective deposition of MoS_x in poly-**1** films by the ion exchange-electroreduction process was also evidenced from UV−vis characterizations (Figure 3). The incorporation by ion-exchange of MoS_4^{2-} anions is evidenced by the rise of a new absorption band at 475 nm (Figure 3, curve b) compared to the dry poly-**1** film (Figure 3, curve a). This is consistent with the visible spectrum of MoS_4^{2-} in water, which is characterized by a strong absorption band (λ_{max} = 467 nm, ε = 12050; Figure 3, curve d).[8] Precipitation of MoS_x in the poly-**1** film following electroreduction of the entrapped MoS_4^{2-} anions is evidenced by a significant increase of the absorption in the near UV and visible regions, with no clear characteristic absorption onset (Figure 3, curve c), as has been previously shown for electrodeposited amorphous MoS_x films.[7,35,39]

AFM measurements in tapping mode were performed to study and compare the morphologies of regular MoS_x deposits and composite films coated on indium tin oxide (ITO) surfaces. Poly-**1**-MoS_x composite films were synthesized using the anion exchange (performed in acetonitrile solution)-potential cycling process. Figure 4 shows topography images of the various surfaces. AFM imaging of the surface of bare ITO presented a homogeneous granular topology (Figure 4A) with a root-mean square roughness (r.m.s.) of 2.5 nm. After modification of the ITO surface with a poly(pyrrole-alkylammonium) film, the topography appeared granular, typical of an electrodeposited poly-**1** film,[28] and the r.m.s. value increased significantly to 10 nm (Figure 4B). The

DOI: 10.1021/acsami.5b03188
ACS Appl. Mater. Interfaces 2015, 7, 15866−15875

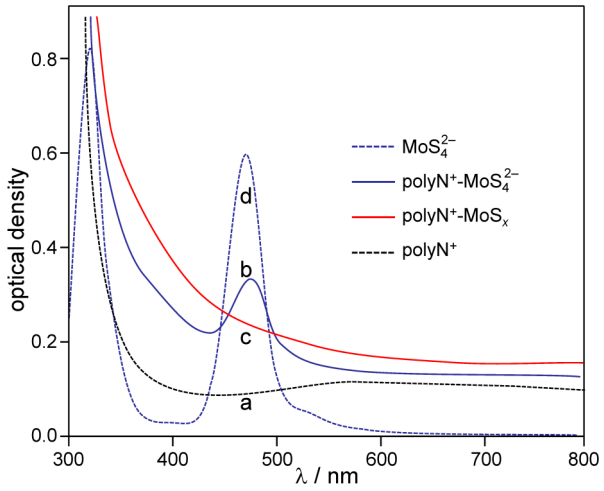

Figure 3. Absorption spectra of (a) a dry poly-**1** film ($\Gamma_{Ru} = 6 \times 10^{-7}$ mol cm^{-2}) coated onto an ITO electrode; (b) the same film soaked for 10 min in a 10 mM aqueous solution of $(NH_4)_2MoS_4$ and thoroughly rinsed, then (c) repeatedly cycled in 0.1 M aqueous $NaClO_4$ electrolyte (pH 6) over the 0.2 to −1.0 V potential range; (d) absorption spectrum of 0.8 mM $(NH_4)_2MoS_4$ in H_2O.

deposition of MoS_x into the poly-**1** film modified electrode is evidenced by the slight change in surface roughness, since the r.m.s. roughness value increased only from 10 nm (Figure 4B) to 16 nm (Figure 4C). The homogeneous dispersion of rather small aggregates of MoS_x particles on the poly**1** film is confirmed by a section analysis of thesurface of the composite (Figure 4G). In contrast the electrodeposition of MoS_x onto naked ITO gave rise to a larger change in topology (Figure 4D). This is reflected by the larger increase in the r.m.s. roughness value up to 25 nm, consistent with the formation on the surface of big aggregates of MoS_x particles with an average diameter of 60 nm (Figure 4H).

All these observations confirm that MoS_x is deposited into the poly**1** matrix, as especially demonstrated by the small increase in the r.m.s value for the film. Moreover, as compared to the coating of a regular film of MoS_x, the electrodeposition of MoS_x into a poly(pyrrole-alkylammonium) film results in the formation of a nanostructured composite, characterized by a more homogeneous distribution of much smaller aggregates of MoS_x particles on its surface.

3.2. Electrocatalytic Reduction of Protons and Hydrogen Evolution at Poly(Pyrrole-alkylammonium)-MoS_x Composite Film Carbon Modified Electrodes. *Tafel Plots.* Tafel plots for proton reduction (Figure 5) have been recorded in acidic (pH 0.3 and pH 1) electrolytes at carbon disc electrodes modified with composite films, synthesized under different experimental conditions, and compared to those obtained with regular amorphous molybdenum sulfide electrodeposits. Tafel slopes and exchange currents are summarized in Table 1. Tafel plots recorded at Clpoly-**1**-MoS_x and ClMoS_x show that the composite film presented the same activity as the amorphous MoS_x film (see Figure 5). Composite and MoS_x film modified electrodes show a behavior compatible with the Tafel equation, with an overpotential for proton reduction varying from 80 to 130 mV at pH 0.3, and from 100 to 150 mV at pH 1, in the 15 μA to 1.5 mA current range.

Tafel slopes for the different cathodes are in the 50−60 mV dec^{-1} range, and the exchange current densities varied from 10^{-7} to 2.3×10^{-7} A cm^{-2} at pH 0.3, and from 4.5×10^{-8} to 12

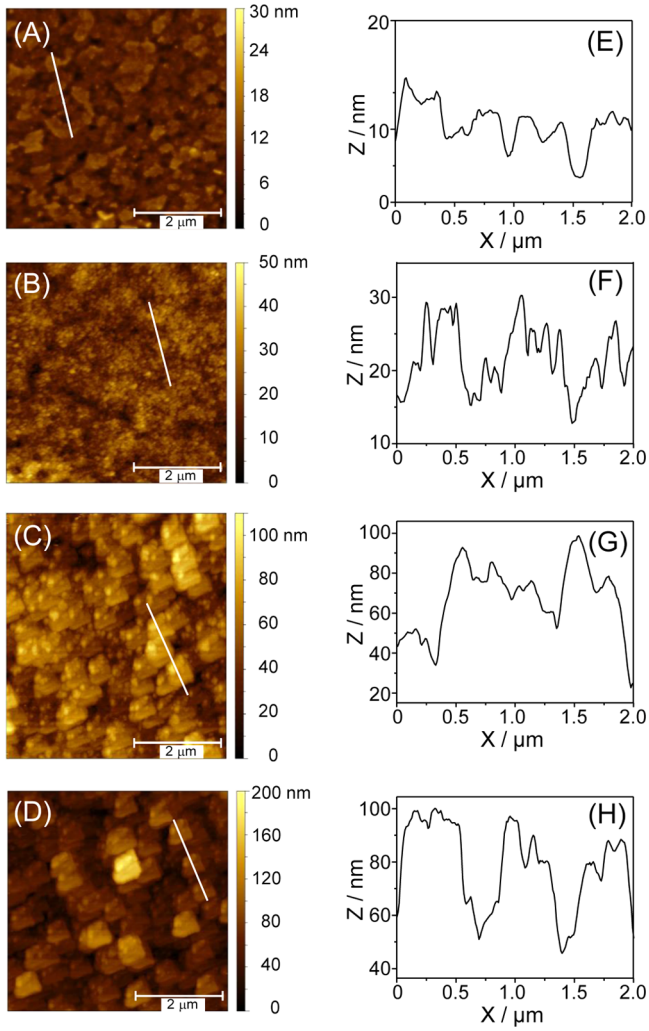

Figure 4. AFM images in tapping mode of (A) a naked ITO surface; (B) ITO surface coated with a poly-**1** film ($\Gamma_{N+} = 2 \times 10^{-8}$ mol cm^{-2}); (C) surface shown in A, after deposition of MoS_x in the poly**1** film, using the ion exchange-electroreduction process in 10 mM $(Et_4N)_2MoS_4$ in CH_3CN, followed by cycling in 0.1 M aqueous $NaClO_4$ ($\Gamma_{N+} = 2 \times 10^{-8}$ mol cm^{-2}; $\Gamma_{MoSx} = 1.2 \times 10^{-8}$ mol cm^{-2}); (D) ITO surface covered with a MoS_x film by repeated CV scans (25 cycles) in a 10 mM solution aqueous solution of $[(NH_4)_2MoS_4]$. Panels E−H present section analysis of the surfaces shown in panels A−D, respectively.

$\times 10^{-8}$ A cm^{-2} at pH 1. The large exchange current densities and relatively small Tafel slopes at the indicated overpotential range demonstrate that the electron transfer rate in the different films is relatively fast, which should be responsible for a high activity of these catalytic electrode materials. Tafel slopes suggest that under these experimental conditions hydrogen evolution proceeds via a fast discharge reaction (Volmer step) and a rate-determining ion + atom reaction (Heyrovsky step),[43] as recently discussed for amorphous MoS_x films[18,44] and nanostructured MoS_x catalysts.[11,20]

Proton Reduction and Hydrogen Evolution at the Preparative Scale. The efficiency of the molybdenum sulfide-based nanocomposite materials for bulk reduction of water at macroscopic electrodes was evaluated using poly-**1**-MoS_x modified carbon foam (0.8 cm^3) electrodes prepared by different experimental conditions, and compared with the electrocatalytic activity of carbon foam modified with regular

DOI: 10.1021/acsami.5b03188
ACS Appl. Mater. Interfaces 2015, 7, 15866−15875

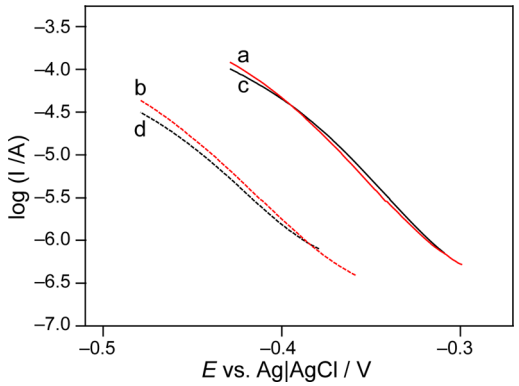

Figure 5. Tafel plots for proton reduction at C|poly-**1**-MoS_x (red curves a and b; electrode synthesized as in Figure 1B; $\Gamma_{N+} = 9 \times 10^{-8}$ mol cm^{-2}; $\Gamma_{MoSx} = 5.4 \times 10^{-8}$ mol cm^{-2}) and C|MoS_x (black curves c and d; electrode synthesized as in Figure S1A with 25 cycles in 10 mM aqueous solution of $(NH_4)_2MoS_4$ containing 0.1 M $NaClO_4$, recorded in aqueous H_2SO_4 at pH 0.3 (solid curves a and c) and pH 1 (dashed curves b and d); ω = 1000 rpm, ν = 5 mV s^{-1}.

Table 1. Tafel Slopes and Exchange Currents[a] for the HER Recorded at Composite Poly1-MoS_x and Amorphous MoS_x Film Modified Carbon Electrodes

electrode[b]	pH	Tafel slope (mV dec^{-1})	exchange current (A cm^{-2})
C|poly-**1**-MoS_x[c]	0.3	51	1.1×10^{-7}
	1	58	8.1×10^{-7}
C|poly-**1**-MoS_x[d]	0.3	54	1.8×10^{-7}
	1	55	4.5×10^{-7}
C|poly**1**-MoS_x[e]	0.3	55	2.3×10^{-7}
	1	56	7.2×10^{-7}
C|MoS_x[f]	0.3	50	1.1×10^{-7}
	1	50	1.2×10^{-7}

[a]Aqueous H_2SO_4 electrolyte. [b]3 mm diameter. [c]Synthesized using the ion exchange (in CH_3CN)-potential cycling (0.1 M $NaClO_4$, pH 6) process; $\Gamma_{N+} = 9 \times 10^{-8}$ mol cm^{-2}; $\Gamma_{MoSx} = 5.4 \times 10^{-8}$ mol cm^{-2}. [d]Synthesized using the ion exchange (in H_2O)-potential cycling (0.1 M $NaClO_4$, pH 6) process; $\Gamma_{N+} = 8 \times 10^{-8}$ mol cm^{-2}; $\Gamma_{MoSx} = 5 \times 10^{-8}$ mol cm^{-2}. [e]Synthesized by 25 CV scans at a C|poly**1** electrode ($\Gamma_{N+} = 1.1 \times 10^{-7}$ mol cm^{-2}) in aqueous $(NH_4)_2MoS_4$. [f]Synthesized by 25 CV scans at a naked C electrode in aqueous $(NH_4)_2MoS_4$.

amorphous MoS_x. Large scale reduction of protons was conducted at −0.3 V vs RHE, the amount of evolved hydrogen being measured by gas chromatography (see Experimental). In all experiments H_2 was produced with quantitative faradaic yields. Electrolyses were arbitrarily stopped after the passage of a fixed charge of 50 to 250 C. The main results of a series of electrolyses are listed in Table 2.

From a general point of view, the composite films presented a much higher catalytic activity and a better operational stability than regular molybdenum sulfide films. The best results were obtained with the cathodes synthesized by anion-exchange incorporation of MoS_4^{2-} in 10 mM aqueous solution of $(NH_4)_2MoS_4$, followed by repeated CV scans over the 0.1 to −1.2 V potential range in clean 0.1 M aqueous $NaClO_4$ electrolyte (pH 6). The initial catalytic current increased with the amount of deposited composite material, from 37 mA (3.3 μmol of MoS_x incorporated into 5.5 μmol of poly**1**; entry 3) to 66 mA (5.6 μmol of MoS_x incorporated into 9.4 μmol of poly**1**; entry 4). A lower activity was obtained with the cathodes synthesized using a 2 mM solution of $(Et_4N)_2MoS_4$ in CH_3CN for the anion exchange step, which gave catalytic currents of 23 mA and 47 mA with composite films based on poly**1** containing 5.0 μmol (entry 1) and 8.8 μmol (entry 2) of ammonium groups, respectively. Moreover, the composite materials prepared via ion exchange by soaking the polymer film modified electrodes in a 10 mM aqueous solution of tetrathiomolybdate have presented a rather good operational stability, as evidenced from current−time curves for HER on the poly**1**-MoS_x modified carbon foam electrodes (see Figure S5 in Supporting Information). For example, with these cathodes the catalytic currents decreased only by 3% and 14% (entry 3; see Figure S5, curve b), and 6% to 11% (entry 4; see Figure S5, curve c) after the consumption of 100 and 250 C, respectively. Under the same experimental conditions, we found that the electrodes synthesized with an anion exchange step performed in acetonitrile were much less stable; the initial catalytic currents decreasing by 22% (entry 1) and 15% (entry 2) after the consumption of 100 C, and up to 25% (entry 2) after the consumption of 250 C (see Figure S5, curve a).

The cathodes prepared by repeated cyclic voltammetry scans of the polymer modified electrodes in a 10 mM aqueous solution of $(NH_4)_2MoS_4$ were characterized by a good catalytic activity and a reasonable operational stability (see entry 5, for

Table 2. Electrocatalytic H_2 Production at Composite Poly-1-MoS_x and Amorphous MoS_x Film Modified Carbon Electrodes[a]

entry	cathode[b]	poly-**1** (μmol)	MoS_x (μmol)[g]	charge consumed (C)	electrolysis time (min)	I_i (mA)[i]	I_f (mA)[j]	TON[k]	TOF[l]
1	C|poly-**1**-MoS_x[c]	5.0	3.0	100	109	23	18	173	95
2	C|poly-**1**-MoS_x[c]	8.8	5.4	100	37	47	40		
				250	103		35	240	140
3	C|poly-**1**-MoS_x[d]	5.5	3.3	100	52	37	36		
				250	122		32	394	194
4	C|poly-**1**-MoS_x[d]	9.4	5.6	100	25	66	62		
				250	67		59	230	206
5	C|poly-**1**-MoS_x[e]	5.6	*h*	110	54	34	31	*h*	*h*
				250	170		24		
6	C|MoS_x[f]		*h*	100	220	9	7	*h*	*h*

[a]In H_2SO_4 electrolyte, pH 0.3; electrolysis at −0.3 V vs RHE. [b]0.8 cm^3 of modified carbon foam (porosity 100 ppi). [c]C|poly-**1** electrode soaked in 2 mM $(Et_4N)_2MoS_4$ in CH_3CN, then repetitively cycled in 0.1 M $NaClO_4$ (pH 6). [d]C|poly-**1** electrode soaked in 10 mM aqueous $(NH_4)_2MoS_4$, then repetitively cycled in 0.1 M aqueous $NaClO_4$ (pH 6). [e]C|poly-**1** electrode directly cycled (25 scans) in 10 mM aqueous $(NH_4)_2MoS_4$. [f]Naked carbon electrode cycled (25 scans) in 10 mM aqueous $(NH_4)_2MoS_4$. [g]Estimated amount of MoS_x deposited, taking into account an incorporation ratio of 60% for MoS_4^{2-} in poly-**1**. [h]Cannot be determined. [i]Initial current. [j]Final current. [k]The mol of H_2 to mol of MoS_x ratio; H_2 was produced with quantitative faradaic yields. [l]Turn over frequency per hour.

DOI: 10.1021/acsami.5b03188
ACS Appl. Mater. Interfaces 2015, 7, 15866−15875

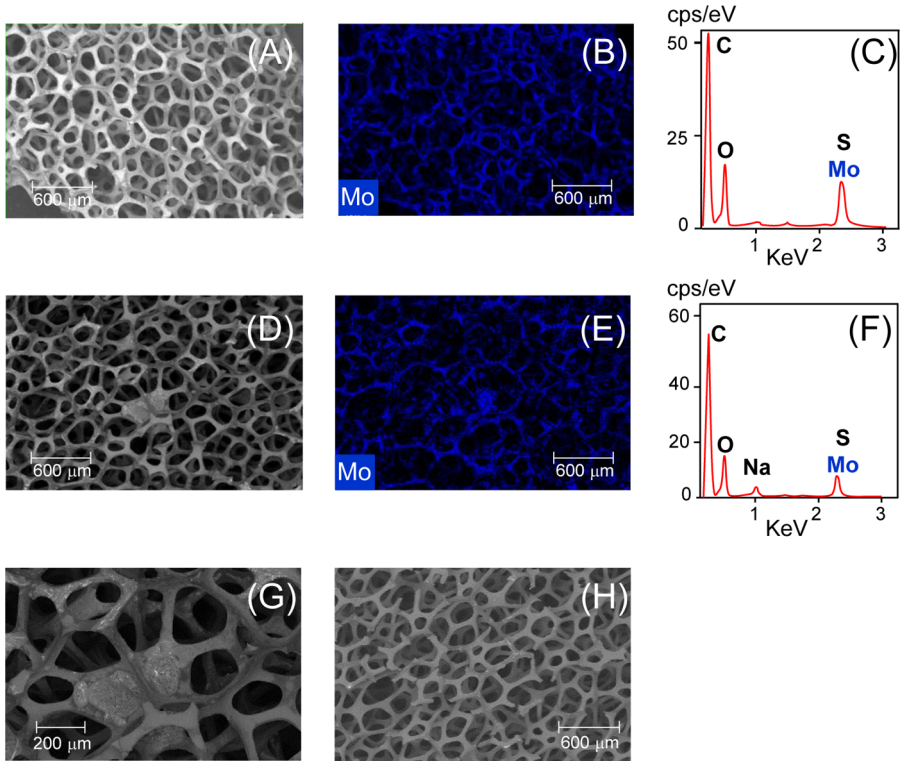

Figure 6. SEM images for carbon foam (100 ppi) surfaces modified with (A) poly-**1**-MoS_x composite and (D) regular amorphous MoS_x films; the electrodeposition of MoS_x on both naked and poly-**1**-modified (5.6 μmol of polymer on 0.8 cm^3 of carbon foam) electrodes was performed with 25 CV scans in a 10 mM aqueous solution of $(NH_4)_2MoS_4$ containing 0.1 M $NaClO_4$, pH 6.6; (G) enlargement of panel B; (B, E) elemental mapping of Mo on panels A and D surfaces, respectively; (C, F) global EDX analysis of panels A and D surfaces, respectively; (H) image of a naked carbon foam surface.

example). However, because of the numerous problems we faced with the deposition process (see the discussion in section 3.1), the clean and less material consuming procedure based on anion-exchange incorporation of MoS_4^{2-} anions into poly-**1** films, followed by their transformation to MoS_x upon repeated CV scans into fresh aqueous electrolyte, obviously appears to be the best method for the electrochemical synthesis of polymer-molybdenum sulfide composite material for HER.

It should be emphasized that naked carbon foam electrodes modified with amorphous MoS_x, upon repeated CV scans in an aqueous solution of $(NH_4)_2MoS_4$ (see section2), have presented a much lower activity than those modified with the poly-**1**-MoS_x composite. A series of experiments performed with five carbon foam|MoS_x electrodes have shown that the initial catalytic currents recorded using the same experimental conditions (pH 0.3, E_{appl} = −0.3 V vs RHE) were only in the 5−9 mA range, and that the operational stability of these cathodes was even lower than that for the composite material. A typical example is depicted in entry 6. This behavior strongly contrasts with that observed for modified carbon disc (3 mm diameter) microelectrodes, which presented similar catalytic activity toward proton reduction when they were coated with composite (see Figure 1C, for example) or regular MoS_x (Figure S1B in Supporting Information) films.

The lower catalytic activity of the carbon foam electrodes modifieds with amorphous MoS_x films cannot be due to a lower amount of catalyst, because we have already observed that the amount of MoS_x deposited using the same experimental conditions by repeated CV scans in an aqueous solution of tetrathiomolybdate anions is significantly higher on naked carbon than on a carbon surface modified by a poly-**1** film (see section 3.1). To try to understand the large difference in catalytic performances of carbon foam electrodes modified with amorphous molybdenum sulfide and polymer-molybdenum sulfide materials, we have studied their morphology by scanning electron microscopy (SEM). We chose to analyze cathodes that have already been used for catalytic experiments, that is, the Cl poly-**1**-MoS_x and ClMoS_x modified carbon foam electrodes, whose performances are presented in entries 5 and 6 of Table 2, respectively. It should be noted that for both cathodes the deposition of MoS_x was performed in the same way, with 25 cyclic voltammetry scans in a 10 mM aqueous solution of $(NH_4)_2MoS_4$. SEM images of these electrodes are shown in Figures 6 and 7. EDX analyses were also performed to decipher the composition and elemental mapping of the samples.

Comparison between the morphology of surfaces covered with poly-**1**-MoS_x composite (Figure 6A) and amorphous MoS_x (Figure 6D) clearly shows that the composite material is more uniformly spread on the carbon network. In the case of the amorphous MoS_x deposit, one can observe the formation of some packs of molybdenum sulfide, which may even block some pores of the sponge (Figure 6G). The more homogeneous distribution of molybdenum catalyst when deposited in the form of a composite material is also revealed by the elemental mapping of the surfaces modified with poly-**1**-MoS_x (Figure 6B) and with amorphous MoS_x (Figure 6E). This observation is corroborated by the global EDX analysis of the surfaces, which shows that the signals for the Mo and S elements is significantly stronger, as compared to the signal of carbon, for the surface covered with the composite material.

Further SEM studies also demonstrate that the electrochemical process allowed the effective deposition of catalytic

DOI: 10.1021/acsami.5b03188
ACS Appl. Mater. Interfaces 2015, 7, 15866−15875

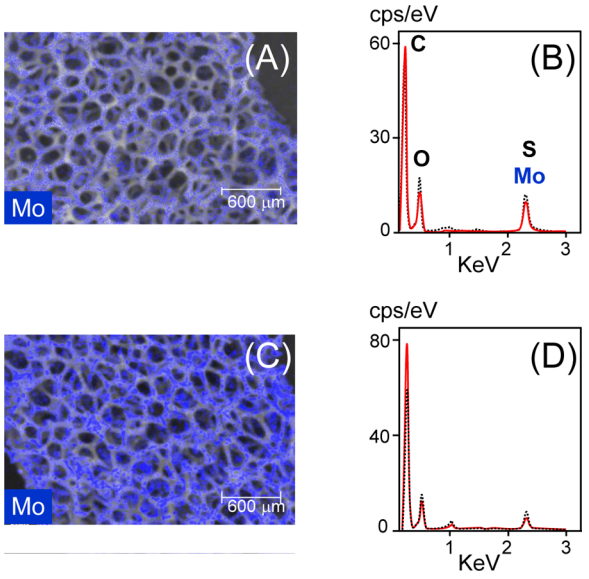

Figure 7. Elemental mapping of Mo on cross sections of carbon foam electrodes modified with (A) poly-**1**-MoS_x composite and (C) amorphous MoS_x; (B, D) global EDX analysis of panels A and C samples, respectively.

materials inside the bulk of the modified carbon foam, as evidenced by the study of cross sections of the electrodes (Figure 7). Elemental mapping of molybdenum (Figure 7A and C) and EDX analysis of the elements (Figure 7B and D) within the foam revealed that the catalyst deposited in the form of a composite is more uniformly spread on the carbon network.

All of these observations suggest that the higher catalytic efficiency of the cathodes synthesized by modification of carbon foam with the poly-**1**-MoS_x composite, as compared to those based on electrodeposited amorphous molybdenum sulfide, is due to a more homogeneous distribution and structuration of the molybdenum catalyst onto and inside the porous carbon network, leading to a higher catalytic surface area-to-volume ratio.

4. CONCLUSION

In conclusion, we have demonstrated that a molybdenum sulfide-polymer nanocomposite synthesized using a straightforward all-electrochemical strategy, by electroprecipitation of MoS_x into a poly(pyrrole-alkylammonium) matrix, is an efficient nanostructured electrode material for electrocatalytic proton reduction and the HER. Electroanalytical investigations have demonstrated that the electron transfer rate in the composite films is fast, which is responsible for a high activity of this cathode material. Bulk electrocatalytic reduction of water at carbon foam modified macroscopic electrodes revealed that the composite films display high catalytic activity and a reasonable operational stability, largely exceeding that of electrodeposited amorphous molybdenum sulfide. The enhanced catalytic performances of the composite electrode material can be attributed to the better structuration and the more homogeneous distribution of the catalyst onto and inside the carbon network, as shown by SEM characterizations. This important finding is similar to that we previously demonstrated for the electrocatalytic oxidation of water using a composite anode elaborated by electrodeposition of iridium oxide nanoparticles into of a poly(pyrrole-alkylammonium) matrix matrix.[33] Therefore, the former and present study reported here demonstrate that this very simple strategy is ideal for making efficient and stable composite electrode materials for water splitting devices. We are currently extending this strategy for the fabrication of composite electrode materials based on functionalized polypyrrole matrices containing catalysts based on earth-abundant metals. Our goal is to apply these new electrode materials to the water splitting reaction, and also to the redox activation of other small molecules, like the electrocatalytic reduction of carbon dioxide for instance.

■ ASSOCIATED CONTENT

Supporting Information

Electrodeposition, electrochemical characterization, and catalytic activity in acidic electrolyte of composite and regular MoS_x film electrodes, and electrochemical characterization of the tetrathiomolybdate anion in acetonitrile electrolyte solution. The Supporting Information is available free of charge on the ACS Publications website at DOI: 10.1021/acsami.5b03188.

■ AUTHOR INFORMATION

Corresponding Author

*E-mail: Jean-Claude.Moutet@ujf-grenoble.fr.

Notes

The authors declare no competing financial interest.

■ ACKNOWLEDGMENTS

The authors thank for funding the French National Agency for Research (Programme LABEX ARCANE, project no. ANR-11-LABX-003). We acknowledge the support from the ICMG FR 2607, and its Chemistry Nanobio Platform for AFM measurements. We thanks T. Bamine for preliminary experiments. Special thanks go to Dr A. J. Gross for a critical reading of the manuscript.

■ REFERENCES

(1) Cook, T. R.; Dogutan, D. K.; Reece, S. Y.; Surendranath, Y.; Teets, T. S.; Nocera, D. C. Solar Energy Supply and Storage for the Legacy and Nonlegacy Worlds. *Chem. Rev.* **2010**, *110*, 6474−6502.

(2) Conway, B. E.; Tilak, B. V. Interfacial Processes Involving Electrocatalytic Evolution and Oxidation of H_2, and the Role of Chemisorbed H. *Electrochim. Acta* **2002**, *47*, 3571−3594.

(3) Laursen, A. B.; Kegnæs, S.; Dahl, S.; Chorkendorff, I. Molydenum Sulfides−Efficient and Viable Materials for Electro- and Photoelectrocatalytic Hydrogen Evolution. *Energy Environ. Sci.* **2012**, *5*, 5577−5591.

(4) Yan, Y.; Xia, B. Y.; Xu, Z.; Wang, X. Recent Development of Molybdenum Sulfides as Advanced Electrocatalysts for Hydrogen Evolution Reaction. *ACS Catal.* **2014**, *4*, 1693−1705.

(5) Morales-Guio, C. G.; Hu, X. Amorphous Molybdenum Sulfides as Hydrogen Evolution Catalysts. *Acc. Chem. Res.* **2014**, *47*, 2671−2681.

(6) Zou, X.; Zhang, Y. Noble Metal-free Hydrogen Evolution Catalysts for Water Splitting. *Chem. Soc. Rev.* **2015**, DOI: 10.1039/C4CS00448E.

(7) Merki, D.; Fierro, S.; Vrubel, H.; Hu, X. Amorphous Molybdenum Sulfide Films as Catalysts for Electrochemical Hydrogen Production in Water. *Chem. Sci.* **2011**, *2*, 1262−1267.

(8) Vrubel, H.; Hu, X. Growth and Activation of an Amorphous Molybdenum Sulfide Hydrogen Evolving Catalyst. *ACS Catal.* **2013**, *3*, 2002−2011.

(9) Benck, J. D.; Chen, Z.; Kuritzky, L. Y.; Forman, A. J.; Jaramillo, T. F. Amorphous Molybdenum Sulfide Catalysts for Electrochemical Hydrogen Production: Insights into the Origin of their Catalytic Activity. *ACS Catal.* **2012**, *2*, 1916−1923.

DOI: 10.1021/acsami.5b03188
ACS Appl. Mater. Interfaces 2015, 7, 15866−15875

(10) Bourgeteau, T.; Tondelier, D.; Geoffroy, B.; Brisse, R.; Laberty-Robert, C.; Campidelli, S.; de Bretignies, R.; Artero, V.; Palacin, S.; Jousselme, B. A H_2-evolving Photocathode Based on Direct Sensitization of MoS_3 with an Organic Photovoltaic Cell. *Energy Environ. Sci.* **2013**, *6*, 2706−2713.
(11) Jaramillo, T. F.; Jørgensen, K. P.; Bonde, J.; Nielsen, J. H.; Horsh, S.; Chorkendorff, I. Identification of Active Edge Sites for Electrochemical H_2 Evolution from MoS_2 Nanocatalysts. *Science* **2007**, *317*, 100−102.
(12) Wang, T.; Liu, L.; Zhu, Z.; Papakonstantinou, P.; Hu, J.; Liu, H.; Li, M. Enhanced Electrocatalytic Activity for Hydrogen Evolution Reaction from Self-Assembled Monodispersed Molybdenum Sulfide Nanoparticles on an Au Electrode. *Energy Environ. Sci.* **2013**, *6*, 625−633.
(13) Bonde, J.; Moses, P. G.; Jaramillo, T. F.; Nørskov, J. K.; Chorkendorff, I. Hydrogen Evolution on Nano-Particulate Transition Metal Sulfides. *Faraday Discuss.* **2009**, *140*, 219−231.
(14) Vrubel, H.; Merki, D.; Hu, X. Hydrogen Evolution Catalyzed by MoS_3 and MoS_2 Particles. *Energy Environ. Sci.* **2012**, *5*, 6136−6144.
(15) Li, Y.; Wang, H.; Xie, L.; Liang, Y.; Hong, G.; Dai, H. MoS_2 Nanoparticles Grown on Graphene: An Advanced Catalyst for the Hydrogen Evolution Reaction. *J. Am. Chem. Soc.* **2011**, *133*, 7296−7299.
(16) Liao, L.; Zhu, J.; Bian, X.; Scanlon, M. D.; Girault, H. H.; Liu, B. MoS_2 Formed on Mesoporous Graphene as a Highly Active Catalyst for Hydrogen Evolution. *Adv. Funct. Mater.* **2013**, *23*, 5326−5333.
(17) Bian, X.; Zhu, J.; Liao, L.; Scanlon, M. D.; Ge, P.; Ji, C.; Girault, H. H.; Liu, B. Nanocomposite of MoS_2 on Ordered Mesoporous Carbon Nanospheres: A Highly Active Catalyst for Electrochemical Hydrogen Evolution. *Electrochem. Commun.* **2012**, *22*, 128−132.
(18) Vrubel, H.; Moehl, T.; Grätzel, M.; Hu, X. Revealing and Accelerating Slow Electron Transport in Amorphous Molybdenum Sulphide Particles for Hydrogen Evolution Reaction. *Chem. Commun.* **2013**, *49*, 8985−8987.
(19) Laursen, A. B.; Vesborg, P. C. K.; Chorkendorff, I. A High-Porosity Carbon Molybdenum Sulphide Composite with Enhanced Electrochemical Hydrogen Evolution and Stability. *Chem. Commun.* **2013**, *49*, 4965−4967.
(20) Chen, Z.; Cummins, D.; Reinecke, B. N.; Clark, E.; Sunkara, M. K.; Jaramillo, T. F. Core−Shell MoO_3−MoS_2 Nanowires for Hydrogen Evolution: A Functional Design for Electrocatalytic Materials. *Nano Lett.* **2011**, *11*, 4168−4175.
(21) Bélanger, D.; Laperrière, G.; Gravel, L. Polypyrrole Films Doped with Tetrathiomolybdate Anions. *J. Electrochem. Soc.* **1990**, *137*, 365−366.
(22) Bélanger, D.; Laperrière, G.; Girard, F.; Guay, D.; Tourillon, G. Physicochemical Characteristics of Electrochemically Deposited Molybdenum Sulfide and Polypyrrole−Tetrathiomolybdate/Molybdenum Strisulfide Composite Electrodes. *Chem. Mater.* **1993**, *5*, 861−868.
(23) Lavallée, S.; Laperrière, G.; Bélanger, D. Electrochemical Preparation of Polypyrrole−Molydenum Trisulfide−Tetratyhiomolybdate Electrode with Various Amounts of Molybdenum Species. *J. Electroanal. Chem.* **1997**, *431*, 219−226.
(24) Wang, T.; Liu, W.; Tian, J.; Shao, X.; Sun, D. Structure Characterization and Conductive Performance of Polypyrrol−Molydenum Sisulfide Intercalation Materials. *Polym. Compos.* **2004**, *25*, 111−117.
(25) Wang, T.; Zhuo, J.; Du, K.; Chen, B.; Zhu, Z.; Shao, Y.; Li, M. Electrochemically Fabricated Polypyrrole and MoS_x Copolymer Films as Highly Active Hydrogen Evolution Electrocatalyst. *Adv. Mater.* **2014**, *26*, 3761−3766.
(26) Shenhar, R.; Norsten, T. B.; Rotello, V. M. Polymer−Mediated Nanoparticle Assembly: Structural Control and Applications. *Adv. Mater.* **2005**, *17*, 657−669.
(27) Coche, L.; Moutet, J.-C. Electrocatalytic Hydrogenation of Organic Compounds on Carbon Electrodes Modified by Precious Metal Microparticles in Redox Active Polymer Films. *J. Am. Chem. Soc.* **1987**, *109*, 6887−6889.
(28) De Oliveira, I. M. F.; Moutet, J.-C.; Hamar-Thibault, S. Electrocatalytic Hydrogenation Activity of Palladium and Rhodium Microparticles Dispersed in Alkylammonium− and Pyridinium−Substituted Polypyrrole Films. *J. Mater. Chem.* **1992**, *2*, 167−173.
(29) Zouaoui, A.; Stephan, O.; Carrier, M.; Moutet, J.-C. Electrodeposition of Copper into Functionalized Polypyrrole Films. *J. Electroanal. Chem.* **1999**, *474*, 113−12.
(30) Cosnier, S.; Deronzier, A.; Moutet, J.-C.; Roland, J.-F. Alkylammonium and Pyridinium Group-Containing Polypyrroles, a New Class of Electronically Conducting Anion-Exchange Polymers. *J. Electroanal. Chem. Interfacial Electrochem.* **1989**, *271*, 69−81.
(31) Rivera, J. F.; Bucher, C.; Saint-Aman, E.; Rivas, B. L.; Aguirre, M. C.; Sánchez, J. A.; Pignot-Paintrand, I.; Moutet, J.-C. Removal of Arsenite by Coupled Electrocatalytic Oxidation at Polymer-Ruthenium Oxide Nanocomposite and Polymer-Assisted Liquid Phase Retention. *Appl. Catal., B* **2013**, *129*, 130−136.
(32) Cosnier, S.; Deronzier, A.; Moutet, J.-C. A Poly[Tris(N-(bipyridylbutyl)pyrrole)-ruthenium(II)]−RuO_2 Catalytic Modified Electrode for Organic Oxidations. *Inorg. Chem.* **1988**, *27*, 2389−2390.
(33) Rivera, J. F.; Pignot-Paintrand, I.; Pereira, E.; Rivas, B. L.; Moutet, J.-C. Iridium Oxide-Polymer Nanocomposite Thin Films for Electrocatalytic Oxidation of Arsenic(III). *Electrochim. Acta* **2013**, *110*, 465−476.
(34) Lattach, Y.; Rivera, J. F.; Bamine, T.; Deronzier, A.; Moutet, J.-C. Iridium Oxide-Polymer Nanocomposite Electrode Materials for Water Oxidation. *ACS Appl. Mater. Interfaces* **2014**, *6*, 12852−12859.
(35) Lattach, Y.; Fortage, J.; Deronzier, A.; Moutet, J.-C. Polypyrrole-Ru(2,2′-bipyridine)$_3^{2+}$/MoS_x Structured Composite Film as a Photocathode for the Hydrogen Evolution Reaction. *ACS Appl. Mater. Interfaces* **2015**, *7*, 4476−4480.
(36) Wolff, T. E.; Berg, J. M.; Hodgson, K. E.; Frankel, R. B.; Holm, R. H. Synthetic Approaches to the Molybdenum Site in Nitrogenase. Preparation and Structural Properties of the Molybdenum-Iron-Sulfur "Double-Cubane" Cluster Complexes $[MoFe_6S_8(SC_2H_5)_9]^{3-}$ and $[MoFe_6S_9(SC_2H_5)_8)]^{3-}$. *J. Am. Chem. Soc.* **1979**, *101*, 4140−4150.
(37) Deronzier, A.; Moutet, J.-C. Polypyrrole Films Containing Metal Complexes: Syntheses and Applications. *Coord. Chem. Rev.* **1996**, *147*, 339−371 and references therein. .
(38) Bélanger, D.; Laperrière, G.; Marsan, B. The Electrodeposition of Amorphous Molybdenum Sulfide. *J. Electroanal. Chem.* **1993**, *347*, 165−183.
(39) Ponomarev, E. A.; Neumann-Spallart, M.; Hodes, G.; Levy-Clément, C. Electrochemical Deposition of MoS_2 Thin Films by Reduction of Tetrathiomolybdate. *Thin Solid Films* **1996**, *280*, 86−89.
(40) Kony, M.; Bond, A. M.; Wedd, A. G. Electrochemistry of Cyanocopper Thiomolybdates and Thiotungstates: Redox-Based Interconversion of Species. *Inorg. Chem.* **1990**, *29*, 4521−4525.
(41) Schäfer, R.; Kaim, W.; Moscherosch, M.; Krejčik, M. Tetrathiorhenate(VI), ReS_4^{2-}. Spectroelectrochemical Characterization (UV−VIS−IR) of a Small New d^1 System and of its Tetrakis(2,2′-bipyridine)diruthenium(II) Complex (EPR). *J. Chem. Soc., Chem. Commun.* **1992**, 834−835.
(42) Moutet, J.-C.; Pickett, C. J. Iron-Sulfur Clusters in Ionic Polymers on Electrodes. *J. Chem. Soc., Chem. Commun.* **1989**, 188−190.
(43) Bockris, J. O'M.; Potter, E. C. The Mechanism of the Cathodic Hydrogen Evolution Reaction. *J. Electrochem. Soc.* **1952**, *99*, 169−186.
(44) Merki, D.; Hu, X. Recent Developments of Molybdenum and Tungsten Sulfides as Hydrogen Evolution Catalysts. *Energy Environ. Sci.* **2011**, *4*, 3878−3888.

DOI: 10.1021/acsami.5b03188
ACS Appl. Mater. Interfaces 2015, 7, 15866−15875